

THE EFFECT OF MODIFIED NATURAL RUBBER COMPATIBILISERS ON POLYAMIDE 6/NATURAL RUBBER BLENDS

F.H. AXTELL, P. PHINYOCHEEP AND P. KRIENGCHIEOCHARN

Department of Chemistry, Faculty of Science, Mahidol University, Rama VI Road, Bangkok 10400, Thailand.

(Received February 5, 1996)

ABSTRACT

Polyamide 6 was blended with natural rubber to provide impact toughness. The blend was compatibilised with maleic anhydride modified natural rubber as a third component in the blends. The modified rubber compatibilised the polyamide 6/natural rubber blends by forming some copolymer between the two phases. The resultant blends had a finer dispersion of natural rubber in the polyamide 6 matrix. Charpy impact strength and tensile properties were improved, giving intermediate performance between polyamide 6 and commercial high impact polyamide 6. The rheological behaviour was affected by the in situ copolymerisation during mixing, with mixing torque increasing as the reaction took place. The polyamide 6 crystallisation was nucleated both by the addition of the natural rubber and by the compatibilisers.

INTRODUCTION

Polyamides toughened by blending with elastomeric impact modifiers have been widely studied. Previous studies have included compatibiliser addition to such immiscible blends. The compatibilisers have been block or graft copolymers having domains compatible with each of the blend's major constituent polymers. The addition of reactive compatibilisers such as maleic anhydride grafted rubber has resulted in improved rubber/polyamide blend properties.¹ Graft copolymers have been formed in situ during processing by a reaction of the functional groups between an anhydride grafted rubber and polyamide 6 chain ends.² The reaction of anhydride units with amine groups at the end of the polyamide chains has been reported as shown in Figure 1.¹

Natural rubber has been reported to increase the impact properties of polyamide 6 if the correct molecular characteristics are used and blending occurs with a viscosity ratio of 0.65.³ In this study the possibility of using graft copolymers of natural rubber and maleic anhydride (NR-g-MAH) to compatibilise the polyamide 6/natural rubber blends to achieve better impact properties was investigated. The resultant blends experienced in situ grafting of the anhydride with the polyamide 6. They had different levels of natural rubber dispersion and varying impact strengths dependent on the level of compatibilisation.⁴

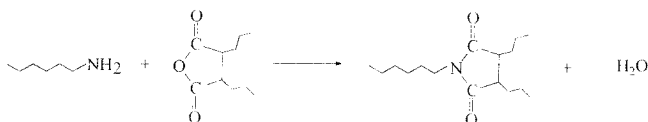


Fig. 1. The reaction of anhydride units with amine groups. (Paul, 1992, (ref. 1))

EXPERIMENTAL

Materials

Commercial grade polyamide 6 (Akulon M223D, Akzo Chemicals b.v.) (PA6) and natural rubber (Thai Technical Rubber TTR5L, Bangkok Rubber Ltd.) (NR) were used in the polymer blends. A commercial grade of high impact polyamide 6 (Akulon K223, Akzo Chemicals b.v.) (HI-PA6) was used as a control material in the study. The compatibilisers based on graft copolymers of maleic anhydride (AR grade, Fluka) (MAH) and NR were prepared in our laboratory using a two stage procedure.

The first compatibiliser, TYPE 1, was prepared by a reaction of MAH with NR. The natural rubber was masticated for 3 minutes on a water cooled two roll mill, then 5% by weight of MAH was added and mixed for 5 minutes; the temperature was controlled below 40° C to avoid sublimation of the MAH. The premixed material was then sheeted off the mill. The premixed material was then mixed in an "in-house" built kneader with a rotor speed of 30 min⁻¹ and a set temperature of 160° C for 5 minute. During this step the graft copolymerisation reaction took place (Reaction (1)) and a chain scission reaction (Reaction (2)) as illustrated in Figure 2. A second compatibiliser, TYPE 2, was prepared in a similar way but using 10% by weight of MAH and kneading for 10 minutes at 160° C. The copolymers prepared were kept in a desiccator prior to characterisation and polymer blending.

Characterisation of NR-g-MAH copolymers by titration

To quantify the extent of grafting that occurred in the kneader mixer, a titration technique was employed to determine the MAH content in the mixed rubber. A thin sheet of NR-g-MAH was soaked in water for 12 hours to remove any unreacted MAH, then dried in a vacuum oven at 60° C for 12 hours. An accurately weighed amount (0.2g) of the dry grafted NR was dissolved overnight in 100ml of a chloroform/toluene mixture (50/50 (% by volume)). An aliquot of the solution (50 ml) was titrated with tetrabutyl ammonium hydroxide in methanol (5 x 10⁻⁵M) by potentiographic titration (Herisau Metrohm E536) at a titration rate of 10ml/min and using the differential mode of operation. For the TYPE 1 copolymer a graft level of 0.75% MAH was found, while the TYPE 2 copolymer showed a graft level of 1.2% MAH.

Polymer blending

The polymer blends prepared had the formulations shown in Table 1. The polymer blending process involved three steps. First the natural rubber was masticated for 3 minutes on a temperature controlled two roll mill at 37° C then NR-g-MAH and antioxidant were added. The mixing was continued for 5 minutes before sheeting off the rubber blend. The second step was the preparation of a masterbatch of the rubber blend in PA6. The sheet of rubber blend was rolled around an equal amount by weight of PA6 pellets (predried at 80° C for 4 hours) giving 65g of material. This was then mixed in an internal mixer (Haake Rheomix 600, with cam D type rotors) at 235° C and a rotor speed of 100 rpm for 10 minutes. The third step was the let down of the masterbatch with dry PA6 to the desired concentration, see Table 1. The blends were identified by a code comprising a number followed by a letter then by another number. The first code number (1 to 7) identifies the NR/MAH-g-NR ratio in the masterbatch. The code letter (A to D) indicates the PA6/masterbatch ratio in the blend. The final number indicates the type of compatibiliser used (1 or 2). The masterbatch and PA6 granules were shaken in a bag then extruded twice through an "in-house" built single screw extruder. A screw speed of 30 rpm and a barrel temperature profile of 190° C - 230° C over 4

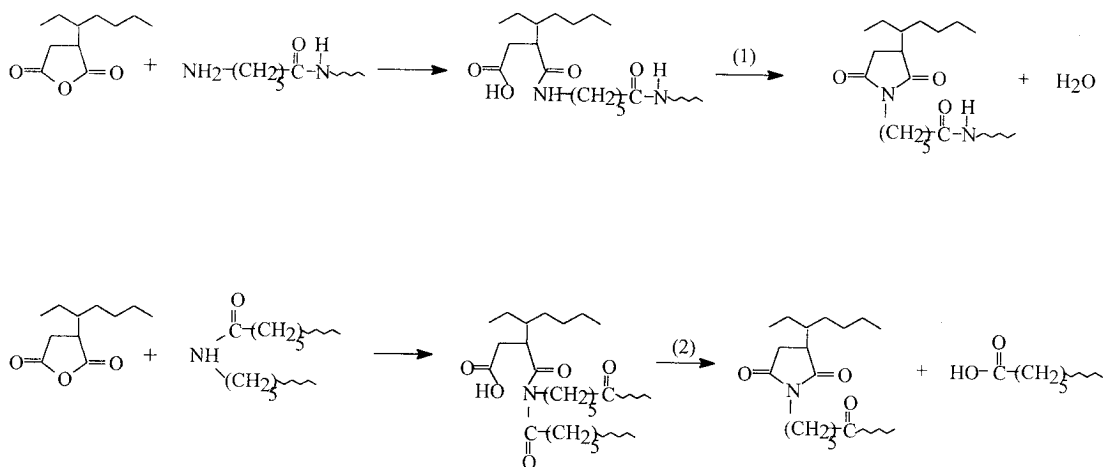


Fig. 2. The reaction between maleic anhydride functionalized rubber and (1) amine group and (2) backbone amide group of PA6 during the blending process.

zones was employed. The screw had a length/diameter ratio of 25:1 and a compression ratio of 2:1. The extrudate was cooled on a metal plate prior to granulation.

Injection moulding

Impact bars

Test specimens for Charpy impact testing were injection moulded using an injection moulding machine (Dr. Boy 22S) fitted with a hopper drier (ERFL Rudolf Zweifel, CH3550) and a two cavity mould for ASTM D256 method B impact bars. An injection pressure of 3.5 bar, a holding time of 15 seconds, a cooling time of 20 seconds, a total cycle time of 50 seconds, a screw rotation speed of 200 rpm and a temperature profile of 225° C to 235° C was used. The specimen bars (125mm x 6.5mm x 12.6mm) were notched after moulding using a broaching tool (Davenport), conforming to ASTM A2436, producing a 45° notch with a 2.4 mm radius.

Tensile dumbbells

A mould having two cavities with different runner and gate configurations was used to prepare side-gated dumbbells, and double-end-gated dumbbells having a weld-line in the testing region of the ISO 527 type B specimens. The specimens were moulded using the same conditions as described above for the impact bars, with adjustments made for the shot volume.

Mechanical Properties

Impact strength

The specimens were tested after conditioning in air for at least 10 days to allow an arbitrary uniform level of moisture uptake to be reached. A Charpy impact tester (Ceast 6545) with a 4 Joule hammer was used for the excess energy test method as described in ASTM D256 method B, 20 samples were tested for each material.

Tensile properties

A universal testing machine (Instron 1026) was used at a crosshead speed of 50mm/min and with a 500kg load cell to determine the tensile strength and elongation at break according to the ISO 527 type B test method. Ten specimens of each type (side-gated and double-end-gated) were tested for each material. The results are shown in Table 2.

TABLE 1. Blend formulations.

Code	PA6 (%)	NR (%)	NR-g-MAH (%)
PA6	100	0	0
HI-PA6	100	0	0
1A	95	5	0
2A1	95	4	1
3A1	95	4.5	0.5
4A1	95	4.75	0.25
1B	90	10	0
2B1	90	8	2
3B1	90	9	1
4B1	90	9.5	0.5
1C	85	15	0
2C1	85	12	3
3C1	85	13.5	1.5
4C1	85	14.25	0.75
1D	80	20	0
2D1	80	16	4
3D1	80	18	2
4D1	80	19	1
1A	95	5	0
2A2	95	4	1
3A2	95	4.5	0.5
4A2	95	4.75	0.25
1B	90	10	0
2B2	90	8	2
3B2	90	9	1
4B2	90	9.5	0.5
1C	85	15	0
2C2	85	12	3
3C2	85	13.5	1.5
4C2	85	14.25	0.75
1D	80	20	0
2D2	80	16	4
3D2	80	18	2
4D2	80	19	1
5D2	80	18.5	1.5
6D2	80	18	2
7D2	80	17.5	2.5

TABLE 2. Mechanical Properties of blends.

Code	Impact Strength (kJm ⁻²)	U.T.S. (MPa)	Elongation at Break (%)	Weld U.T.S. (MPa)	Weld Elongation at Break (%)
PA6	7.1	72.3	331	63.2	269
HI-PA6	37.0	29.6	120	36.5	172
1A	9.8	38.7	123	36.8	115
2A1	13.6	47.3	202	42.9	164
3A1	16.1	41.8	160	38.6	73
4A1	16.5	43.3	199	36.6	107
1B	11.3	33.9	117	30.2	99
2B1	16.4	42.6	206	38.3	193
3B1	18.5	32.6	130	31.4	65
4B1	16.9	35.8	161	36.9	125
1C	13.5	30.2	84	27.9	41
2C1	19.2	34.0	139	31.1	53
3C1	19.8	32.9	119	28.3	38
4C1	17.1	29.1	112	29.8	66
1D	14.7	26.3	76	29.1	31
2D1	19.8	29.2	128	27.3	36
3D1	19.0	33.9	90	23.4	48
4D1	16.5	27.9	136	26.4	82
1A	9.8	38.7	123	36.8	115
2A2	18.3	49.2	236	44.9	184
3A2	17.3	49.8	260	43.1	223
4A2	16.9	43.6	164	39.9	152
1B	11.3	33.9	117	30.2	99
2B2	20.1	34.4	193	36.2	128
3B2	19.8	42.8	226	37.8	179
4B2	19.7	41.6	217	35.7	135
1C	13.5	30.2	84	27.9	41
2C2	20.2	34.7	183	32.8	124
3C2	20.2	35.4	200	33.8	180
4C2	21.2	33.9	168	33.1	131
1D	14.7	26.3	76	29.1	31
2D2	23.0	28.2	181	25.4	122
3D2	24.3	30.9	75	26.6	61
4D2	21.4	28.0	118	31.4	193
5D2	25.1	30.6	125	29.5	108
6D2	21.8	31.1	140	29.7	132
7D2	24.9	30.8	154	29.0	99

Morphology of blends

Scanning electron microscopy

The fracture surfaces of an impact bar, broken after immersion in liquid nitrogen for 2 hours, were etched with toluene for 2 days at room temperature to dissolve any unbound rubber from the specimen surface. The specimens were dried in a vacuum oven at 60° C overnight, then sputter coated with gold. The morphology of the blends was examined by scanning electron microscopy (SEM) (Hitachi S2500) at 2,000x magnification. Photomicrographs of the blend morphology show the dispersion of the NR particles in the PA6 matrix, see Figures 3-5. From the photomicrographs, measurements of the hole diameters (d_i) gave the NR particle size distributions for the different blends. From these data the number average diameter ($\langle d_n \rangle$) and weight average diameter ($\langle d_w \rangle$) were determined using equation (1) and (2).⁵

$$\langle d_n \rangle = \frac{\sum n_i d_i}{\sum n_i} \quad (1)$$

$$\langle d_w \rangle = \frac{\sum n_i d_i^2}{\sum n_i d_i} \quad (2)$$

Molecular orientation

Shrinkage testing

To determine the extent of frozen-in molecular orientation in the PA6 and the blends resulting from the flow during injection moulding, shrinkage tests were conducted on side gated tensile dumbbells. The lengths of four tensile dumbbells were measured after moulding and then again after annealing at 90° C for 2 hours in an oven. Measurements of their length were made after the specimens had cooled down to room temperature. The shrinkage due to relaxation of the molecular orientation in the amorphous regions of the PA6 was determined. If shrinkage had been significant it would imply that the molecular orientation may have affected the mechanical properties of the materials. For the PA6 the shrinkage was 0.07%, for the binary blends the values were in the range 0.14% (1B) to 0.32% (1A), for the TYPE 1 compatibilised blends the range was 0.13% (3D1) to 0.24% (2C1) and for the TYPE 2 compatibilised blends the range was 0.11% (4C2) to 0.41% (7D2). As the results showed close to zero shrinkage, it was confirmation that the moulding conditions used produced specimens free of significant molecular orientation in the amorphous phases.

PA6 crystallisation

To determine whether the rubber and compatibiliser affected the PA6 crystallisation behaviour, differential scanning calorimetry (DSC) was conducted. Samples (~10 mg) were cut from the end of the impact bars at the same position on each specimen. The samples were sealed in aluminium pans and were analysed in the DSC (Perkin Elmer DSC-7). The heating curve was measured at a scan rate of 10° C/minute from 50° C to 260° C. The samples were held at 260° C for 5 minutes then cooled to 50° C at 10° C/minute to obtain the cooling (exothermic) curves. The heats of fusion and crystallisation were obtained from the areas below the heating (endothermic) peaks and above the cooling (exothermic) peaks, respectively. Heat of fusion or crystallisation of the PA6 phase (ΔH_{PA6}) in the blends were calculated by using equation (3):

$$\Delta H_{PA6} = \Delta H_{blend} / \Phi_{PA6} \quad (3)$$

Where ΔH_{blend} is the heat of fusion or crystallisation of the blend as determined from the DSC analysis and Φ_{PA6} is the weight fraction of PA6 in the blend. The results are shown in Table 4.

Melt rheology

To indicate changes due to chemical interactions or molecular degradation in the blends, rheological measurements were made. The mixing torque of the PA6, NR (masticated for 8 minutes), and their blends were recorded during preparation of the blends in the internal mixer (Haake Rheomix 600) at different mixing times. The torque results from 7 batches were averaged for the blends and the average of duplicate batches for the neat polymers, as shown in Table 5.

Molau test for blend compatibility

The blends were immersed in formic acid for more than 2 weeks. The turbidity of the solutions was used as an indicator of the occurrence of any chemical compatibilising copolymer (CCC).⁶ Any CCC would give a turbid solution. The solutions showed some turbidity, indicating that CCC was present. The binary blends also showed some turbidity, indicating that some grafting occurred between the oxidised NR and the PA6.

FTIR characterisation

Fourier transform infrared spectroscopy (FTIR) was used to determine the chemical nature of compatibilisation and of any chemical degradation that occurred. Samples were prepared by immersing the blends in toluene to dissolve the NR and CCC; the PA6 phase did not dissolve and hence it could be separated by filtration. A film was cast from the filtrate onto a potassium bromide cell and dried with hot air. FTIR (Perkin Elmer FTIR system 2000) spectra were collected with a resolution of 1cm^{-1} for 24 scans. The presence of absorption peaks associated with PA6 such as amine and carbonyl units ($1520\sim 1570\text{cm}^{-1}$) would indicate strong interactions between CCC and PA6 in the extracted rubber specimen. Another possible source for a carbonyl absorption peak could be from thermooxidative degradation of the NR (but this would be at a different wave number, $\sim 1620\text{cm}^{-1}$). As PA6 is insoluble in toluene, attenuated total reflectance (ATR) was used to get the spectrum of PA6 from an impact bar with a resolution of 1cm^{-1} and 24 scans.

RESULTS AND DISCUSSION

Evidence of chemical compatibilising copolymer (CCC) formation in PA6/NR-g-MAH/NR blends

Cimmino *et al.*⁷ found that impact strength and elongation at break of PA6/EPR blends increased when compatibiliser was added because chemical compatibilising copolymer (CCC) was formed during blending. The reaction of the anhydride groups of the NR-g-MAH and the amide and amine groups of the PA6 resulted in the chemical compatibilising copolymer (CCC);⁵ consequently adhesion between the two phases was increased. The occurrence of CCC in the blends prepared with both the TYPE 1 and TYPE 2 compatibilisers was verified by the Molau test and the FTIR traces, see Figure 6. The CCC increased the compatibility of the blend components and stabilized the blend morphology, reducing dispersed phase ripening during cooling after cessation of mixing due to lower interfacial tension. Therefore the thermodynamic driving force moves towards minimisation of surface area, and hence interfacial tension, is reduced.

The FTIR spectrum of the dissolved NR after the in situ reaction to form the CCC showed the presence of peaks for the amine ($3200\text{-}3400\text{ cm}^{-1}$) and carbonyl (1720 cm^{-1}) groups from the PA6 which had reacted to form part of the reaction copolymer CCC, see Figure 6. The PA6 did not dissolve in the toluene and thus was not present in a free state in the FTIR sample. The amine stretching peak (between $1647\text{-}1654\text{ cm}^{-1}$) and carbonyl stretching peak of PA6 (between $1539\text{-}1558\text{ cm}^{-1}$) were observed in the reacted rubber. Also NR thermooxidation increased the carbonyl stretching peak at 1720 cm^{-1} which would lead to increased compatibility of the NR with the PA6 by hydrogen bonding.

Effect of NR-g-MAH compatibiliser and rubber content on mechanical properties of PA6/NR blends

Table 2 shows that the TYPE 1 compatibiliser (NR-g-MAH with 0.75% grafted MAH) increased the impact strength to higher values than the corresponding binary blends, up to 68% higher in the case of blend 4A1 compared to blend 1A. Increases in elongation at break and stress at break were also observed, see Table 2. The moulded-in weld line caused a decrease in the elongation at break in the PA6 and blend samples, but not in blend 4D2 or the HI-PA6 samples. With the TYPE 1 compatibiliser, the impact strength increased with compatibiliser loading until an optimum amount of 10% NR-g-MAH copolymer in the masterbatch; after this the impact strength decreased. The higher amount of compatibiliser increased the weld line elongation at break and stress at break only at rubber contents up to 10%. At higher rubber levels the compatibiliser did not affect the properties. The impact strengths of the blends compatibilised with the TYPE 1 compatibiliser, up to 19.8 kJ/m^2 were typically double that of the unmodified PA6 (7.1 kJ/m^2); but half the value of the commercial HI-PA6 (37.0 kJ/m^2). This is a significant improvement in the impact behaviour of unmodified PA6 achieved by compatibilised melt blending and hence offers an alternative production route to the reactor process for commercially manufacturing HI-PA6.

The blends containing the TYPE 1 compatibiliser had a lower number average particle size of NR particles, as measured from the SEM photomicrographs, than the blends that did not contain any compatibiliser, except for blend 4D1, see Table 3 and Figures 3 & 4. The chemical compatibilisation and possibly some interactions of a physical nature stabilised the morphology of the blends, inhibiting coalescence of the dispersed phase during secondary processing, such as injection moulding. Coalescence of dispersed rubber particles has been reported to occur during injection moulding for binary (non-compatibilised) blends.³

The TYPE 2 compatibiliser (NR-g-MAH with 1.2% grafted MAH) showed the same evidence for CCC formation as observed in the case of the TYPE 1 compatibiliser, but the blends had even better properties. The blends containing TYPE 2 compatibiliser had impact strengths up to 25.1 kJ/m^2 , for blend 5D2, i.e. over triple that of the unmodified PA6 (7.1 kJ/m^2) and reached 68% of the impact strength of the HI-PA6. These compatibilised blends had up to 87% higher impact strengths, e.g. 18.3 kJ/m^2 for blend 2A2, than the comparable binary blend 1A (9.8 kJ/m^2). For all blends containing the TYPE 2 compatibiliser, impact strength increased with both rubber and compatibiliser content. The blends having low rubber contents, exhibited elongations at break up to 260%, e.g. for blend 3A2, i.e. 210% higher than the HI-PA6 and 79% of the unmodified PA6. The tensile strengths were also good, e.g. 49.8 MPa for blend 3A2 (68% higher than HI-PA6), and 69% of the PA6 value. Greater compatibiliser content increased the weld line elongation at break and stress at break for the blends containing low levels of unmodified NR.

The TYPE 2 compatibiliser resulted in all blends having NR particles of lower number

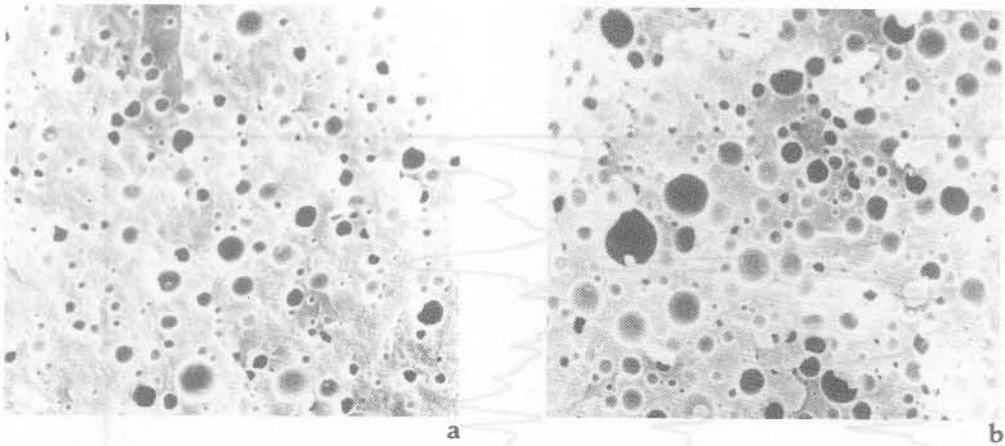


Fig. 3. SEM micrographs of uncompatibilised PA6/NR blends (a) blend 1B (90/10); (b) blend 1D (80/20). Scale marking shows 15 microns.

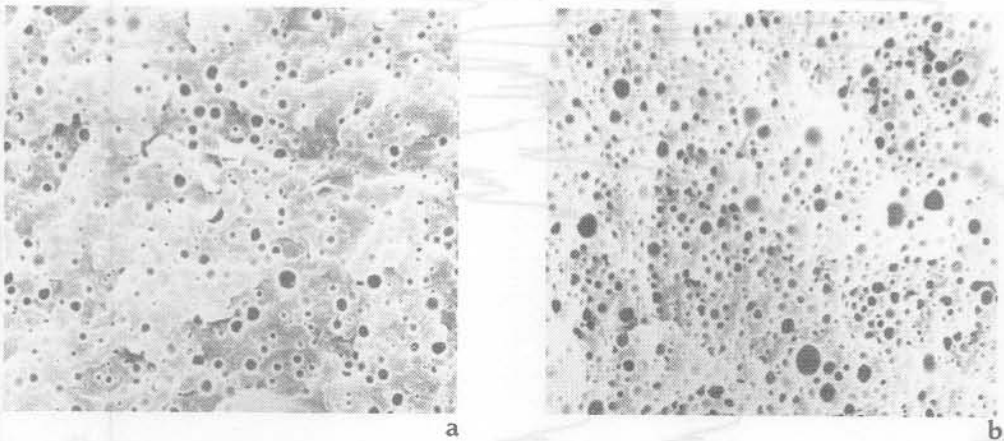


Fig. 4. SEM micrographs of PA6/NR-g-MAH/NR blends using TYPE 1 compatibiliser (0.75% MAH grafting) (a) blend 2B1 (90/2/8); (b) blend 2D1 (80/4/16). Scale marking shows 15 microns.

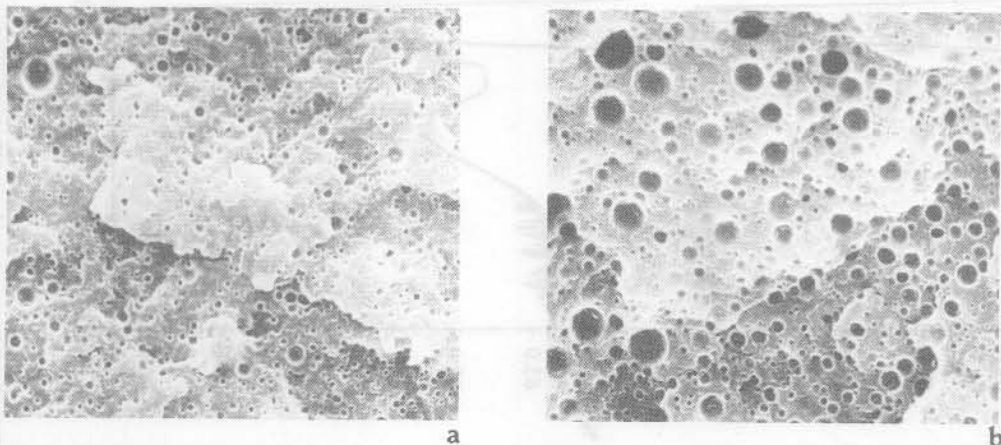


Fig. 5. SEM micrographs of PA6/NR-g-MAH/NR blends using TYPE 2 compatibiliser (1.2% MAH grafting) (a) blend 2B2 (90/2/8); (b) blend 2D2 (80/4/16). Scale marking shows 15 microns.

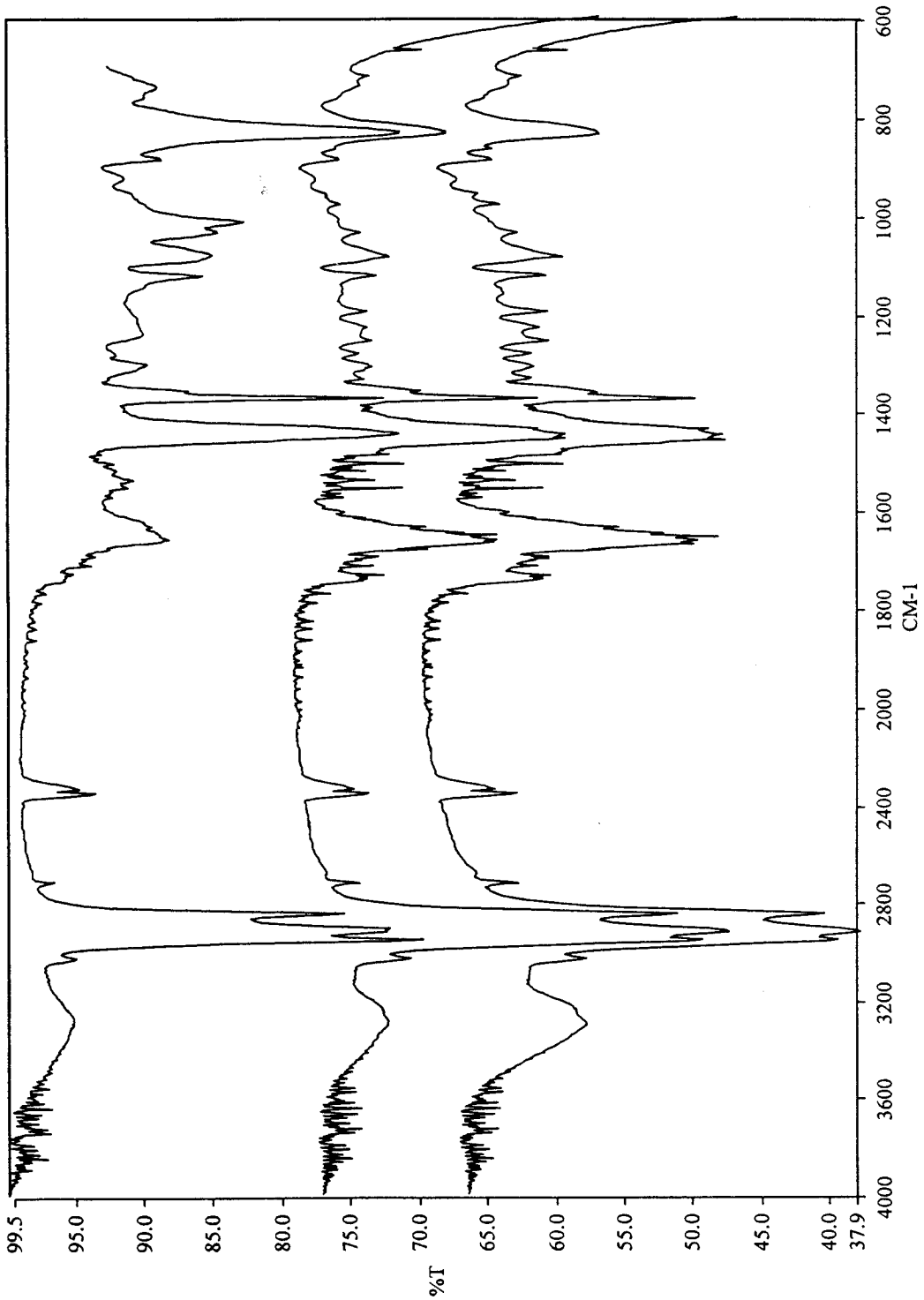


Fig. 6. FTIR spectra of (a) NR (upper spectrum), (b) PA6/NR blend with TYPE 1 compatibiliser (middle spectrum), (c) PA6/NR blends with TYPE 2 compatibiliser (lower spectrum). Note peaks for the amine (3200-3400 cm⁻¹) and carbonyl (1720 cm⁻¹) units.

TABLE 3. Particle size distributions of NR in compatibilised PA6/NR blends.

Code	Min. d (microns)	Max. d (microns)	$\langle d_n \rangle$ (microns)	$\langle d_w \rangle$ (microns)	$\langle d_w \rangle / \langle d_n \rangle$
1A	0.17	2.73	1.24	1.51	1.22
2A1	0.17	1.19	0.50	0.66	1.30
3A1	0.17	2.90	1.04	1.30	1.25
4A1	0.17	4.27	1.37	1.74	1.27
2B1	0.17	2.73	0.95	1.18	1.24
3B1	0.17	3.41	1.21	1.66	1.37
4B1	0.17	4.09	1.29	1.76	1.36
1C	0.17	4.60	1.35	1.71	1.27
2C1	0.17	3.41	1.10	1.33	1.21
3C1	0.17	5.11	1.39	1.88	1.35
4C1	0.17	5.28	1.22	1.80	1.47
1D	0.17	5.46	1.47	2.10	1.43
2D1	0.17	2.39	0.90	1.14	1.27
3D1	0.17	3.75	1.25	1.67	1.34
4D1	0.17	9.20	1.19	2.33	1.96
1A	0.17	2.73	1.24	1.51	1.22
2A2	0.17	1.19	0.41	0.62	1.53
3A2	0.17	1.53	0.50	0.66	1.31
4A2	0.17	4.26	1.02	1.36	1.34
1B	0.17	4.27	1.37	1.74	1.27
2B2	0.17	3.75	0.67	0.96	1.43
3B2	0.17	2.22	0.86	1.09	1.27
4B2	0.17	1.71	0.69	0.84	1.23
1C	0.17	4.60	1.35	1.71	1.27
2C2	0.17	2.73	0.62	0.93	1.51
3C2	0.17	2.22	0.76	1.04	1.37
4C2	0.17	3.41	0.81	1.20	1.48
1D	0.17	5.46	1.47	2.10	1.43
2D2	0.17	4.26	1.04	1.65	1.58
3D2	0.17	2.56	0.76	1.05	1.38
4D2	0.17	3.75	0.91	1.39	1.53
5D2	0.17	2.90	0.86	1.23	1.43
6D2	0.17	3.75	0.78	1.16	1.48
7D2	0.17	2.73	0.86	1.18	1.38

TABLE 4. Thermal Analysis of blends.

4(a) DSC Heating curve analysis - Melting peak

Code	From (°C)	To (°C)	Peak (°C)	Onset (°C)	Area (J/g)	<d _n > (micron)	<d _w > (micron)
PA6	151.4	239.4	206.1	203.8	99.7	-	-
1A	159.0	228.5	213.0	204.3	87.8	1.24	1.51
1B	175.0	217.4	209.7	199.4	71.6	1.37	1.74
1C	153.8	227.6	212.8	201.7	91.5	1.35	1.74
3C2	156.0	222.9	206.0	202.7	86.6	0.76	1.04
1D	156.3	217.4	209.2	205.9	78.7	1.47	2.10
3D1	177.0	217.0	208.9	200.4	67.7	1.25	1.67
3D2	176.0	221.8	210.7	205.8	71.6	0.76	1.05
6D2	177.7	220.0	210.3	204.9	70.5	0.78	1.16

4(b) DSC Cooling curve analysis - Crystallisation peak

Code	From (°C)	To (°C)	Peak (°C)	Onset (°C)	Area (J/g)	<d _n > (micron)	<d _w > (micron)
PA6	123.9	187.6	177.2	181.4	64.7	-	-
1A	130.8	181.1	177.1	181.3	64.4	1.24	1.51
1B	125.9	186.9	176.8	180.7	66.2	1.37	1.74
1C	133.8	187.2	177.2	181.2	65.9	1.35	1.74
3C2	128.8	186.9	177.6	181.8	67.9	0.76	1.04
1D	137.0	187.9	177.5	181.2	64.8	1.47	2.10
3D1	126.5	189.5	178.2	181.6	65.6	1.25	1.67
3D2	128.8	187.9	178.1	181.8	66.8	0.76	1.05
6D2	134.8	188.9	177.9	181.6	66.2	0.78	1.16

TABLE 5. Haake Rheometer mixing torque (metres/gram) for compatibilised PA6/NR blends during blending at 235° C

Code	1 min.	2 min.	3 min.	4 min.	5 min.	10 min.	15 min.	20 min.	25 min.
PA6	462	286	223	216	200	179	192	190	218
NR	655	496	439	416	392	359	333	296	273
1A	273	112	86	76	81	91	109	130	161
2A1	341	169	143	133	122	122	114	122	120
3A1	296	182	146	135	135	140	133	140	143
4A1	309	174	128	127	117	104	107	133	138
1B	374	117	107	107	104	96	107	112	122
2B1	314	167	148	138	130	130	125	130	138
3B1	278	171	148	143	138	135	138	138	133
4B1	236	143	107	104	112	78	86	86	86
1C	252	115	107	101	99	86	96	88	83
2C1	315	193	161	154	159	146	156	156	146
3C1	289	151	138	127	130	117	109	114	83
4C1	231	120	112	112	101	76	78	76	86
1D	213	107	102	96	94	78	76	73	78
2D1	273	164	154	148	153	138	122	122	125
3D1	185	96	104	104	107	115	122	99	83
4D1	223	148	127	117	125	109	101	102	88
1A	273	112	86	76	81	91	109	130	161
2A2	301	128	96	94	81	83	86	91	83
3A2	296	143	122	112	104	99	106	104	114
4A2	216	104	73	62	57	63	57	52	63
1B	374	117	107	107	104	96	107	112	122
2B2	312	197	153	130	135	143	135	123	109
3B2	322	171	138	143	138	83	81	104	91
4B2	210	94	55	52	47	55	65	68	67
1C	252	115	107	101	99	86	96	88	83
2C2	281	159	138	135	133	104	99	96	93
3C2	210	120	101	94	106	68	65	68	65
4C2	179	73	55	49	52	52	39	52	65
1D	213	107	102	96	94	78	76	73	78
2D2	218	138	128	122	117	94	81	86	81
3D2	156	68	55	57	55	47	42	39	29
4D2	192	104	91	91	83	78	70	70	78
5D2	226	107	88	88	78	75	73	86	73
6D2	189	114	99	91	89	80	70	70	73
7D2	223	122	133	138	135	133	109	109	115

average diameter and weight average diameter and narrower range of number average particle size than the binary blends, except blend 4A2.

Comparison of TYPE 1 and TYPE 2 compatibilisers shows that the higher percentage grafting gave better toughness to the blends resulting from higher levels of CCC formation, and hence increased the compatibility of the two blend phases in a similar manner to that reported by Greco *et al.*⁸ The stress at break and elongation at break of blends containing TYPE 2 compatibiliser were higher than those containing TYPE 1 compatibiliser. This result was not observed by Greco *et al.* [8] and so the NR-g-MAH in this study gave a better level of compatibilisation of PA6/NR than the EPR-g-MAH compatibiliser in PA6/EPR. The TYPE 2 compatibilised blends had lower number average diameters and weight average diameters than the TYPE 1 compatibilised blends, see Figures 3-5 and Table 3. This observation verifies that the PA6/NR blends were effectively compatibilised by the NR-g-MAH copolymers, and that TYPE 2 was more effective than TYPE 1.⁵ These compatibilised PA6/NR blends had intermediate toughness behaviour between commercial PA6 and HI-PA6.

Effect of NR-g-MAH compatibiliser on the rheological properties of PA6/NR blends

After the NR-g-MAH was added to the blends, higher torque values were observed than those for the uncompatibilised binary blends. This indicates that some chemical reaction occurred between the anhydride functionalised NR with the amide and amine groups of the PA6 giving copolymers or some physical interactions occurred increasing the torque value of the blends. Higher torque values were obtained with addition of TYPE 2 than with TYPE 1 copolymer due to a greater amount of CCC being formed, as reported in the work of Greco *et al.*^{8,9}

From the torque data shown in Table 5 the mixing torque of the blends showed a sharp decrease at the beginning of mixing due to the heating and fluxing of the cold materials. After this the torque was slightly reduced due to degradation of the PA6 and NR. At high temperatures thermal oxidation of the NR occurred giving some functionality to the NR.¹⁰ This functionalised NR interacted with the PA6 giving copolymers, which had a higher molecular weight than the neat polymers, and so had a higher torque value than the binary blends, see Table 5 for the values after 10 minutes (for blends 2A1, 3A1, 2B1, 3B1, 2C1, 3C1, 2D1, 3D1, 4D1, 2B2, 2C2, 2D2 and 7D2).

The ratio of torque values at 10 minutes and 4 minutes for the blends containing NR-g-MAH were all lower than 0.63. This indicates that the anhydride grafted NR increased the amount of degradation of the PA6 by acidolysis¹¹ and/or degradation of the rubber phases.

With the NR-g-MAH as the compatibiliser, the TYPE 1 copolymer increased the torque values to the highest of all the blends. The increase of torque after 15 minutes was observed in the blends with low rubber and low compatibiliser content (batches 3A1, 4A1 and 4A2). In contrast, the high percentage grafting of the TYPE 2 copolymer reduced the torque to lower than that for the binary blends. This was due to the increased degradation of the PA6 by the acidolysis reaction. Borggreve and Gaymans⁵ also suggested that during blending the MAH grafted on the EPDM reacted with the amide groups of the PA6 and chain scission occurred.

Effect of NR-g-MAH compatibiliser on PA6 crystallisation in PA6/NR blends

From the DSC results shown in Table 4 (a) it can be seen that with the compatibilisers added to the PA6, narrower fusion peaks were observed indicating a more uniform crystalline texture, and a smaller peak area for the PA6 melting peak (enthalpy of fusion). The onset of fusion peaks occurs at a higher temperature than for the PA6 and the binary blends, suggesting a different crystalline form may be predominant in the compatibilised specimens as moulded.

For the crystallisation behaviour as determined by DSC cooling at 10° C/minute the trends are different to the fusion peak analysis, showing that the crystalline texture is dependent on the cooling conditions that were different in the injection moulding of the impact bars, than the carefully controlled cooling of a small amount of material in the DSC instrument. The crystallisation peaks for the TYPE 1 compatibilised blends showed that the modified rubber acted as a nucleating agent for the PA6, resulting in wider peaks, of larger area for the cooling curves (enthalpy of crystallisation) indicating a greater degree of crystallinity, also the onset of the peaks occurs at a higher temperature than for the TYPE 2 compatibilised blends, and both compatibilisers gave blends of higher crystallinity than the PA6 and the binary blends. The smaller diameters of the NR droplets in the compatibilised blends yield larger surface areas where nucleation can occur. Similar results have been reported for the binary blends³ and for blends of PA6/EPM-g-MA/EPM.^{7,8,9} The mechanical properties of the compatibilised blends show improvements in elongation at break which result from the in situ copolymerisation and not from the higher degree of crystallinity.

CONCLUSIONS

In this work natural rubber was grafted with maleic anhydride by simple heat and shear initiation, this caused degradation and therefore chain scission resulted in free radicals that could initiate the anhydride grafting. This was achieved in a conventional intensive mixer, without any peroxide initiator present. The blends of PA6 and NR were compatibilised by the NR-g-MAH copolymers. The blend compatibilisation occurred by physical interactions and by chemically creating in situ copolymers, chemical compatibilising copolymers (CCC), as verified by the observations from the Molau test, FTIR spectra, and the increased mixing torque. Addition of the compatibiliser gave a higher degree of dispersion, resulting in smaller particle size range of the rubber phase. The smaller rubber particles present gave greater toughness to the blends, with improved mechanical properties including Charpy impact strength, tensile strength and elongation at break. The compatibilised blends produced have industrially interesting property combinations intermediate between those of PA6 and commercial HI-PA6. This offers the possibility for natural rubber producing countries to modify PA6 cost effectively for applications requiring tough engineering plastics, without the need to import the more expensive toughened grades such as HI-PA6. The compatibilisers acted as nucleating agents for the PA6, giving different crystalline texture than the binary blends.

ACKNOWLEDGMENTS

The authors would like to acknowledge the National Metals and Materials Technology Center (MTEC), National Science and Technology Development Agency (NSTDA) for the research grant awarded to them for this work. Also, we would like to thank R.Venables for his comments.

REFERENCES

1. Paul, D.R., (1992), *Proceedings of the International Symposium on Polymer Alloys and Composites (ISPAC)*, 9-11 December 1992, Hong Kong Polytechnic, 21-37.
2. Triacca, V.J., Ziaee, S., Barlow, J.W., Keskkula, H., and Paul, D.R., (1991), *Polymer*, **32**, 1401-1413.
3. Axtell, F.H., Phinyocheep, P., and Monthachitra, P., (1992), *J. Sci. Soc. Thailand*, **18**, 195-215.
4. Kriengchieocharn, P., (1993), "A study of the influence of modified natural rubber on polyamide 6/natural rubber blends", *M.Sc. thesis, Mahidol University*.
5. Borggreve, R.J.M. and Gaymans, R.J., (1989), *Polymer*, **30**, 63-70.
6. Curto, D., Valenza, A., and La Mantia, F.P., (1990), *J. Appl. Polym. Sci.*, **39**, 865-873.
7. Cimmino, S., Coppola, F., D'Orazio, L., Greco, R., Maglio, G., Malinconico, M., Mancarella, C., Martuscelli, E., and Ragosta, G., (1986), *Polymer*, **27**, 1874-1884.
8. Greco, R., Malinconico, M., Mancarella, C., Martuscelli, E., Ragosta, G., and Scarinzi, G., (1987), *Polymer*, **28**, 1185-1189.
9. Greco, R., Malinconico, M., Mancarella, C., Martuscelli, E., Ragosta, G., and Scarinzi, G., (1988), *Polymer*, **29**, 1418-1425.
10. Hrivikova, J. and Blazkova, A., (1980), *J. Appl. Polym. Sci.*, **25**, 761-769.
11. Fettel, E.M., (1964), "Chemical reactions of polymers", John Wiley & Sons, New York, 610-612.